

Spiraling elliptic breathers in saturable nonlinear media with linear anisotropy

Guo Liang,¹ Qi Guo,^{1,*} Qian Shou,¹ and Zhanmei Ren¹

¹*Laboratory of Nanophotonic Functional Materials and Devices,
South China Normal University, Guangzhou 510631*

compiled: November 15, 2017

We have introduced a class of spiraling elliptic breathers in saturable nonlinear media with linear anisotropy. Two kinds of evolution behaviors of the breathers, rotating and pendulum-like librating, are both predicted by the variational approach, and confirmed by the numerical simulation. The spiraling elliptic breathers can rotate even though they have no initial orbital angular momentum (OAM). Due to the linear anisotropy of the media, the OAM is no longer conserved. Therefore, the angular velocity is found to be not a constant but a periodic function of the propagation distance. When the linear anisotropy is large enough, the spiraling elliptic breathers can librate like the pendulum. The spiraling elliptic breathers exist in the media with not only the saturable nonlinearity but also the nonlocal nonlinearity, as a matter of fact, they are universal in the nonlinear media with the linear anisotropy.

OCIS codes: (190.6135) Spatial solitons; (190.3270) Kerr effect.
<http://dx.doi.org/10.1364/XX.99.099999>

1. Introduction

The self-trapping and self-focusing of optical beams in nonlinear media of both linear isotropy (isotropic diffraction) and nonlinear isotropy have been studied extensively for over three decades [1–3]. In an isotropic medium, the circular symmetry is conserved, and therefore the fundamental solitons have circularly-symmetrical shape. Introducing the nonlinear anisotropy into the medium, the self-trapping beams with ellipse-shaped spots can be obtained. Coherent elliptic strongly nonlocal solitons were observed experimentally in lead glass [4], where the nonlinear anisotropy is achieved by rectangular boundaries in the transverse. Elliptical discrete solitons can form in an optically induced two-dimensional photonic lattice, where the nonlinear anisotropy comes of enhanced photorefractive anisotropy and nonlocality under a nonconventional bias condition [5]. It was reported recently that the anisotropic nonlocal nonlinearity of the diffusive (thermal) type can stabilize the dipole-mode solitons, which are completely unstable in the isotropic medium [6].

The linear anisotropy is also important in many soliton phenomena. In Ref.[7], the self-focusing of the beam propagating in any direction in uniaxial crystals was discussed, there exists an elliptic self-trapping beam for the extraordinary light in uniaxial crystals. Stationary elliptic quadratic solitons [8] and elliptic nonlocal solitons [9] were found successively in biaxial crystals and

the nematic liquid crystals with large birefringence, respectively. The generation of multiple solitons [10, 11] were reported theoretically and experimentally to be the consequence of the linear anisotropy. The linear isotropy can also make the elliptic optical beams without the initial orbital angular momentum (OAM) rotate during the linear propagation [12], and the rotation angle will monotonously approach to the value determined by the media and the input parameters of the beam. It was predicted very recently that the spiraling elliptic solitons with the OAM can exist in isotropic saturable nonlinear media [13] and in isotropic nonlocal nonlinear media [14], where the OAM can bring in the effective linear anisotropy. The nonlinear propagation of elliptic optical beams in saturable nonlinear medium with the linear anisotropy is investigated in the paper. A class of spiraling elliptic breathers is found to exist in such media, which can rotate even though they have no initial OAM. The angular velocity is no longer a constant but a periodic function of the propagation distance. The libration of the spiraling elliptic breathers like the pendulum is discovered when the linear anisotropy of the media is large enough.

2. The variational solution of the spiraling elliptic breathers

The propagation of optical beams in saturable nonlinear media with linear anisotropy can be modeled by the

* Corresponding author: guoq@sncu.edu.cn

following nonlinear Schrödinger equation (NLSE) [2, 7]

$$i\frac{\partial A}{\partial \zeta} + \frac{1}{2k} \left(\alpha_1^2 \frac{\partial^2 A}{\partial \xi^2} + \alpha_2^2 \frac{\partial^2 A}{\partial \eta^2} \right) + \frac{kn_2}{n_0} \frac{I}{1 + I/I_s} A = 0, \quad (1)$$

where $A(\xi, \eta, \zeta)$ is a paraxial beam, $I = |A|^2$ is the beam intensity, I_s is the saturation intensity, n_2 is the nonlinear index coefficient, ζ is the longitudinal coordinate, ξ and η are the transverse coordinates, k is the wavenumber in the media without nonlinearity, n_0 is the linear refractive index of the media, α_1 and α_2 are the diffraction coefficients along ξ and η directions, respectively. The larger the coefficients are, the more strongly the optical beam diffracts in those directions. When $\alpha_1 = \alpha_2$, an optical beam of the circular shape will diffract equally along any direction [14]. But here we consider the case of linear anisotropy, i.e., $\alpha_1 \neq \alpha_2$. Introducing the scaled dimensionless variables as $x = \xi/w_0, y = \eta/w_0, z = \zeta/L_d, \varphi = \left(\frac{kn_2 L_d}{n_0}\right)^{1/2} A$, where $L_d = 2kw_0^2$ is the Rayleigh distance, equation (1) takes the form of

$$i\frac{\partial \varphi}{\partial z} + \alpha_1^2 \frac{\partial^2 \varphi}{\partial x^2} + \alpha_2^2 \frac{\partial^2 \varphi}{\partial y^2} + \frac{|\varphi|^2}{1 + |\varphi|^2/\gamma} \varphi = 0, \quad (2)$$

where γ is the dimensionless saturation intensity, and $\gamma = 1$ is assumed in the paper. Through the variable transformation $X = x/\alpha_1, Y = y/\alpha_2, Z = z$, the NLSE (2) becomes

$$i\frac{\partial \varphi}{\partial Z} + \frac{\partial^2 \varphi}{\partial X^2} + \frac{\partial^2 \varphi}{\partial Y^2} + \frac{|\varphi|^2}{1 + |\varphi|^2} \varphi = 0, \quad (3)$$

where the optical beam is changed to $\varphi(X, Y, Z)$. The Lagrangian of equation (3) can be expressed as [13] $L = i/2 \iint (\varphi^* \partial \varphi / \partial Z - \varphi \partial \varphi^* / \partial Z) dXdY - H$, where H is the Hamiltonian of the system,

$$H = \iint \left(\left| \frac{\partial \varphi}{\partial X} \right|^2 + \left| \frac{\partial \varphi}{\partial Y} \right|^2 - |\varphi|^2 + \ln(1 + |\varphi|^2) \right) dXdY. \quad (4)$$

We introduce a trial function [13],

$$\varphi = \sqrt{\frac{P}{\pi b(Z)c(Z)}} G \left[\frac{\xi}{b(Z)} \right] G \left[\frac{\eta}{c(Z)} \right] \exp(i\phi), \quad (5)$$

where the Gaussian envelope is $G(t) = \exp(-t^2/2)$, the phase is $\phi = B(Z)\xi^2 + \Theta(Z)\xi\eta + Q(Z)\eta^2 + \theta(Z)$, $\xi = X \cos \beta(Z) + Y \sin \beta(Z)$, $\eta = -X \sin \beta(Z) + Y \cos \beta(Z)$ and $P = \iint |\varphi|^2 dXdY$ is the power. From equation (5), we can obtain the OAM, $M = \text{Im} \iint \varphi^* (X \frac{\partial \varphi}{\partial Y} - Y \frac{\partial \varphi}{\partial X}) dXdY = 1/2 P (b^2 - c^2) \Theta$. Inserting the trial solution (5) into the Lagrangian, L can be analytically determined. By using the variational approach [15] we can obtain that $P' = 0, H' = 0, M' = 0, \beta' = 2(b^2 + c^2)\Theta/(b^2 - c^2)$ and $b' = 4bB, c' = 4cQ$, where

the primes indicate derivatives with respect to the variable Z . Inserting relational expressions above into the Hamiltonian (4), we obtain

$$H = \frac{P}{8} (b^2 + c^2) + \Pi, \quad (6)$$

where $\Pi = \frac{P}{2} \left[\frac{1}{b^2} + \frac{1}{c^2} + 4\sigma^2 \frac{b^2 + c^2}{(b^2 - c^2)^2} \right] - \pi bc Li_2 \left(-\frac{P}{\pi bc} \right) - P$ is the potential of the system with $\sigma = M/P$. Here, $Li_2(t)$ is the dilogarithm function, defined by $Li_2(t) = \int_t^0 dq \ln(1 - q)/q$. Solitons are corresponding to the extremum of the potential $\Pi(b, c)$. So letting $\partial \Pi / \partial b = \partial \Pi / \partial c = 0$, we obtain

$$\frac{4}{b^3} + \frac{16b\sigma^2(b^2 + 3c^2)}{(b^2 - c^2)^3} + \frac{4\pi c}{P} F(b, c) = 0, \quad (7)$$

$$\frac{4}{c^3} - \frac{16c\sigma^2(3b^2 + c^2)}{(b^2 - c^2)^3} + \frac{4\pi b}{P} F(b, c) = 0, \quad (8)$$

where $F(b, c) = \left[\ln \left(1 + \frac{P}{\pi bc} \right) + Li_2 \left(-\frac{P}{\pi bc} \right) \right]$. If b and c are given, the critical power and the critical OAM can be obtained from equations (7) and (8), with which the optical beam can propagate keeping its elliptic profile changeless and rotating stably in the XYZ -coordinate frame. The rotational angular velocity can be obtained as

$$\omega = \beta' = \frac{4\sigma(b^2 + c^2)}{(b^2 - c^2)^2}. \quad (9)$$

Then, we can obtain $\beta(Z) = \omega Z + \beta_0$, where β_0 is the initial inclination of the elliptic optical beam at $Z = 0$ in the XYZ -coordinate frame. Here, we give an example that [13], when $b = 4.26, c = 2.13$ the critical power $P = 127.32\pi$, the critical OAM $\sigma = 0.35$, and the rotational angular velocity $\omega = 0.17$. The optical beam expressed in the xyz -coordinate frame (the laboratory frame) is of the form

$$\varphi = \sqrt{\frac{P}{\pi bc}} \exp \left[-\frac{\left(\frac{x \cos \beta}{\alpha_1} + \frac{y \sin \beta}{\alpha_2} \right)^2}{2b^2} - \frac{\left(\frac{y \cos \beta}{\alpha_2} - \frac{x \sin \beta}{\alpha_1} \right)^2}{2c^2} \right] \times \exp \left[i\Theta \left(\frac{x \cos \beta}{\alpha_1} + \frac{y \sin \beta}{\alpha_2} \right) \left(\frac{y \cos \beta}{\alpha_2} - \frac{x \sin \beta}{\alpha_1} \right) + i\theta \right] \quad (10)$$

The evolution of the optical beam in the xyz coordinate system, as an example, is shown in figure 1, where the input beam is expressed as equation (10) and $\alpha_1 = 1.0, \alpha_2 = 1.3$. The optical beam rotates during the propagation, while its shape changes periodically. To confirm the validity of the approximately analytical solution, we compare the two half widths obtained from variational solution, $w_x = \alpha_1 (b^{-2} \cos^2 \omega_c z + c^{-2} \sin^2 \omega_c z)^{-1/2}$ and $w_y = \alpha_2 (c^{-2} \cos^2 \omega_c z + b^{-2} \sin^2 \omega_c z)^{-1/2}$, with those from the numerical simulation of equation (2), we find an excellent agreement as shown in figure 2. The method of numerical simulation used here is the split-step Fourier method [16] by using equation (10) as the input beam at $z = 0$.

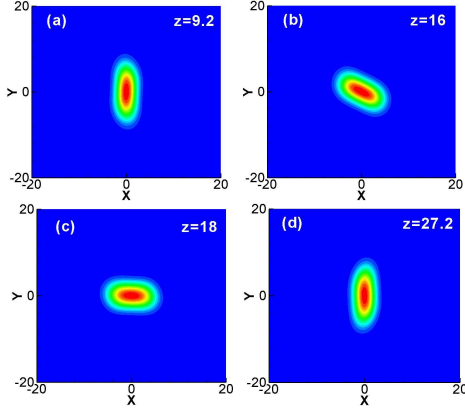


Fig. 1. (color online) Propagation of the spiralling optical breather. The parameters are $\alpha_1 = 1.0, \alpha_2 = 1.3, b = 4.26, c = 2.13, P = 127.32, \Theta = 0.052, \beta_0 = 0$ and $\theta = 0$.

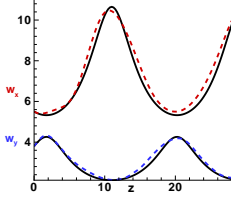


Fig. 2. (color online) Comparison of the beam width of the analytical solution (black solid curves) with that of the numerical simulation (red dashed curves for w_x and blue dashed curves for w_y). The parameters are the same as those in figure 1.

3. Rotation mode

Now we pay attention to the rotation of the spiralling elliptic breathers in the media with the linear anisotropy. To this end, we should transform the expression of the elliptic optical beam, equation (10), to its standard elliptic form through the rotation of coordinates by the angle ϑ . We can obtain that $\tan(2\vartheta) = \frac{\gamma_{xy}}{\gamma_{xx} - \gamma_{yy}}$, where $\gamma_{xx} = (b^{-2} \cos^2 \beta + c^{-2} \sin^2 \beta) / \alpha_1^2$, $\gamma_{yy} = (b^{-2} \sin^2 \beta + c^{-2} \cos^2 \beta) / \alpha_2^2$ and $\gamma_{xy} = 2 \sin \beta \cos \beta (b^{-2} - c^{-2}) / (\alpha_1 \alpha_2)$. One of the semi-axes of the standard elliptic optical spot is

$$w_b = \sqrt{\frac{1}{\gamma_{xx} \cos^2 \vartheta + \gamma_{yy} \sin^2 \vartheta + \gamma_{xy} \sin \vartheta \cos \vartheta}}, \quad (11)$$

the other is

$$w_c = \sqrt{\frac{1}{\gamma_{xx} \sin^2 \vartheta + \gamma_{yy} \cos^2 \vartheta - \gamma_{xy} \sin \vartheta \cos \vartheta}}. \quad (12)$$

From equations (11) and (12), it is found that the two semi-axes of the elliptic optical beam vary with the propagation distance z for the general case of $\alpha_1 \neq \alpha_2$ and $b \neq c$. No spiralling elliptic solitons exist in the model

(2), but only spiralling elliptic breathers exist, the semi-axes of which vary with z periodically. For the case of $\alpha_1 = \alpha_2$, from equations (11) and (12) we can obtain $w_b = \alpha_1 c, w_c = \alpha_1 b$, which is the case of Ref.[13] that the spiralling elliptic solitons can form in the saturable nonlinear media with linear isotropy, rotating with a constant angular velocity. For the case of $b = c$, we can obtain $\vartheta(z) = 0$, that is, the two semi-axes of the elliptic solitons lie on the x and y axes all the time. There is no rotation. It is the case of Ref.[7], where an elliptic self-trapping beam for the extraordinary light is found to exist in the uniaxial crystal and the semi-axes of the elliptic optical beam lies on the principal plane of the uniaxial crystal.

The angular velocity of the optical beam in the xyz -coordinate frame can be obtained as

$$\varpi = \frac{d\vartheta}{dz} = \frac{f_1(b, c, \omega, \alpha_1, \alpha_2, z)}{f_2(b, c, \omega, \alpha_1, \alpha_2, z)}, \quad (13)$$

where $f_1(b, c, \omega, \alpha_1, \alpha_2, z) = \alpha_1 \alpha_2 (b^2 - c^2) \omega [(\alpha_1^2 + \alpha_2^2)(b^2 - c^2) + (\alpha_1^2 - \alpha_2^2)(b^2 + c^2) \cos 2(\omega z + \beta_0)]$ and $f_2(b, c, \omega, \alpha_1, \alpha_2, z) = 2(\alpha_1^2 b^2 - \alpha_2^2 c^2)^2 \cos^4(\omega z + \beta_0) + 2(\alpha_2^2 b^2 - \alpha_1^2 c^2)^2 \sin^4(\omega z + \beta_0) + [\alpha_1^2 \alpha_2^2 (b^4 + c^4) + (\alpha_1^4 - 4\alpha_1^2 \alpha_2^2 + \alpha_2^4) b^2 c^2] \sin^2 2(\omega z + \beta_0)$. The angular velocity ϖ is a periodic function of z but not a constant, which is shown in figure 3 (a). We can prove that $f_2 \geq 0$ in

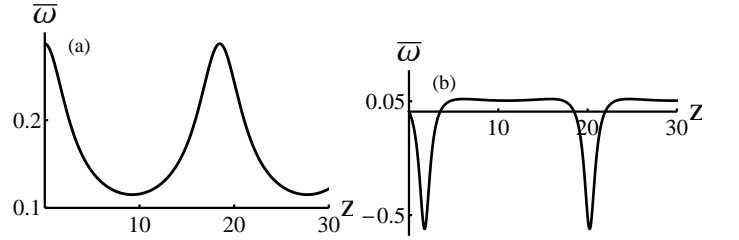


Fig. 3. Variation of rotational angular velocity with propagation distance. The parameters are the same as those in figures 1 and 2 for (a), and the parameters for (b) are $b = 4.26, c = 2.13, P = 127.32, \Theta = 0.052, \alpha_1 = 2.5, \alpha_2 = 1.0, \beta_0 = 73^\circ$.

equation (13). If f_1 is always positive or negative at any propagation distance z , the spiralling elliptic breathers will rotate anticlockwise or clockwise. Mathematically, positive f_1 at any z only requires that the minimum of f_1 is positive, i.e., $\min(f_1) \geq 0$. Similarly, negative f_1 at any z only requires that the maximum of f_1 is negative, i.e., $\max(f_1) \leq 0$. From this we can obtain the criteria for the rotation of the spiralling elliptic breathers as $\min(\rho, 1/\rho) \leq \rho_M \leq \max(\rho, 1/\rho)$ but $\rho_M \neq 1$, where $\rho = b/c$, and $\rho_M = \alpha_1/\alpha_2$ is the parameter of the linear anisotropy of the media. The larger is the difference between ρ_M and 1, the larger is the linear anisotropy of the media. We find that f_1 is always positive when $\min(\rho, 1/\rho) \leq \rho_M \leq \max(\rho, 1/\rho)$, that is, the spiralling elliptic breather will rotate anticlockwise when the linear anisotropy of the media is small enough. As a

matter of fact, we have used the positive ω here, which makes f_1 always positive. Of course, we can also use a negative ω , then the spiraling elliptic breather will rotate clockwise when $\min(\rho, 1/\rho) \leq \rho_M \leq \max(\rho, 1/\rho)$. From equation (9), it can be found that the sign of ω depends on sign of σ . But the signs of σ have no effects on equations (7) and (8). Taking parameters $b = 4.26, c = 2.13, \alpha_1 = 1.0$ and $\alpha_2 = 1.3$ as an example, we can find the parameter ρ_M satisfy $1/\rho < \rho_M < 1$, then can predict the spiraling elliptic breathers will rotate anticlockwise, which is confirmed by figures 1 and 3 (a).

The OAM of the optical beam in the xyz -coordinate frame is obtained as $m = \text{Im} \iint \varphi^* (x \frac{\partial \varphi}{\partial y} - y \frac{\partial \varphi}{\partial x}) dx dy = \frac{P \Theta f_1(b, c, \omega, \alpha_1, \alpha_2, z)}{4 \omega \alpha_1 \alpha_2 (b^2 - c^2)}$. If we set $f_1(z = 0) = 0$, the spiraling breathers will have no initial OAM. Meanwhile, by setting $\min(f_1) = 0$ or $\max(f_1) = 0$, the spiraling breathers without the initial OAM will rotate anticlockwise or clockwise. Then we obtain that the spiraling breathers without the initial OAM rotate anticlockwise when $\rho_M = 1/\rho, \beta_0 = 0$, as is shown in figure 4, and rotate clockwise when $\rho_M = \rho$ and $\beta_0 = \pi/2$. Such rotation of the spiraling elliptic breathers without the initial OAM in the media with the linear anisotropy is different from the rotation resulting from the initial OAM in the isotropy media [4, 14].

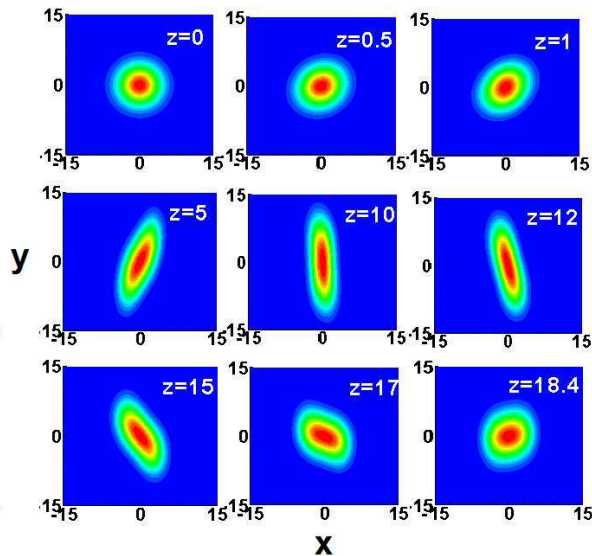


Fig. 4. (color online) Evolution of spiraling optical breather in one period. The parameters are the same as those in figure 1 except for $\alpha_1 = 1, \alpha_2 = 2$ so that $\rho_M = 1/\rho$.

From the expression of the spiraling elliptic breathers, equation (10), we can obtain the period of the evolution as $T = \pi/\omega$. Then the period of the spiraling elliptic breather in figure 4 is about 18.4, where $\omega = 0.17$, but we find that the shape of the the spiraling elliptic breather after a period is not the same as the input one at $z = 0$. It is mainly because that the exact solutions of NLSE (2)

are not the Gaussian function, the variational approach will bring in deviations if we take the Gaussian trial solution like equation (5). The deviations will be expected to disappear if we use the numerical iterative solution of NLSE (2) as the input beam at $z = 0$. Nonetheless, we can correctly predict the behaviors of the rotation and libration of the spiraling elliptic breathers by using the variational approach.

4. Pendulum-like libration mode

If we increase the linear anisotropy of the media so that $\rho_M > \max(\rho, 1/\rho)$ or $\rho_M < \min(\rho, 1/\rho)$, the angular velocity ϖ will change its sign during the propagation of the spiraling elliptic breathers, that is, the direction of the rotation of the spiraling elliptic breathers will change, and the libration will appear, librating back and forth like the pendulum, which is shown in figures 3 (b) and 5. The spiraling breather rotates clockwise from $z = 0$ to $z = 3$, then changes the rotational direction and rotate anticlockwise until $z = 17$. The critical angle, at which the rotation direction changes, can be found as

$$\tan(2\vartheta_c) = \frac{1 - \rho^2}{\sqrt{\rho^2 - 1 - \rho^4 + \rho^2 \rho_M^2}}. \quad (14)$$

When $\rho = 2, \rho_M = 2.5$, the critical angle can be obtained to be -25° , which agrees well with that of the numerical simulation, as is shown in figure 5 (d).

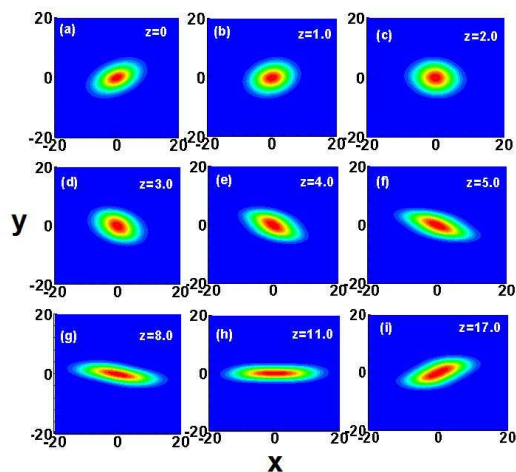


Fig. 5. (color online) Evolution of the spiraling optical breather. The parameters are the same as those in figure 3 (b).

It can be proved that the OAM is not conserved by the NLSE with unequal diffraction coefficients, so the libration of the spiraling elliptic breathers is universal in the nonlinear media with the linear anisotropy if the anisotropy is large enough. For example, apart from the saturable nonlinear media, we can simply explore the libration of the spiraling elliptic breathers in nonlocal nonlinear media with the linear anisotropy. We simulate the nonlocal nonlinear

Schrödinger equation $i\frac{\partial\varphi}{\partial z} + \alpha_1^2\frac{\partial^2\varphi}{\partial x^2} + \alpha_2^2\frac{\partial^2\varphi}{\partial y^2} + \varphi \int \int R(x-y)|\varphi(x',y')|^2 dx dy = 0$ taking the optical beam (10) as an input beam with the response function of the media $R = 1/(2\pi w_m^2) \exp[-(x^2 + y^2)/(2w_m^2)]$, where the parameters, $w_m = 15, b = 2, c = 1, P = 1.25 \times 10^5, \Theta = 0.374$, are the same as those in the figure 1 (a) of Ref.[14]. But instead of $\alpha_1 = \alpha_2 = \frac{\sqrt{2}}{2}$ in [14], here we use the diffraction coefficients $\alpha_1 = \frac{5\sqrt{2}}{8}$ and $\alpha_2 = \frac{\sqrt{2}}{4}$ to make sure that the parameter of the linear anisotropy, $\rho_M = 2.5$, and $\rho = b/c = 2$ are the same as those in figure 5 of this paper. The evolution of the spiraling elliptic breather is shown in figure 6, where the libration happens too. The spiraling breather rotates anticlockwise from $z = 0$ to $z = 6$, then changes the rotational direction and rotate clockwise until $z = 13$, then changes the rotational direction again, and rotate anticlockwise until $z = 19$, then changes the rotational direction again, and rotate clockwise until $z = 25.6$. The shape of the spiraling elliptic breather at $z = 25.6$ after one period is almost the same as that of the input beam at $z = 0$. The larger the degree of nonlocality is, the less the difference of the shapes between the beam after one period and the input beam is. The details about the rotation and libration of the spiraling elliptic breathers in nonlocal nonlinear media with the linear anisotropy will not be reported herein.

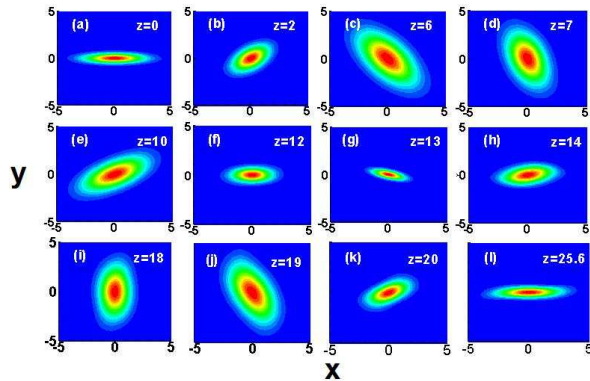


Fig. 6. (color online) Evolution of the spiraling optical breather in one period. The parameters are the same as those in figure 1 (a) of [14] except that the diffraction coefficients in the x and y directions of equation (2) of [14] are $\frac{5\sqrt{2}}{8}$ and $\frac{\sqrt{2}}{4}$.

5. Conclusion

We have introduced a class of spiraling elliptic breathers in saturable nonlinear media with linear anisotropy. The breathers have the elliptic light spots, and have two dif-

ferent kinds of evolution modes, that is, the rotation mode and the pendulum-like mode. The spiraling elliptic breathers can rotate even though they have no initial orbital angular momentum. Due to the anisotropy of the media, the angular velocity is not a constant but a periodic function of the propagation distance. When the anisotropy of the media is large enough, the spiraling elliptic breathers will librate like the pendulum. The spiraling elliptic breathers are universal in the nonlinear media with the linear anisotropy, such as the saturable nonlinear media, the nonlocal nonlinear media and so on. The predictions of the rotation and libration of the spiraling elliptic breathers by the variational approach are confirmed by the numerical simulation.

ACKNOWLEDGMENTS

This research was supported by the National Natural Science Foundation of China (Grant Nos. 11074080, 11274125), and the Natural Science Foundation of Guangdong Province of China (Grant No. S2012010009178).

References

- [1] S. Trillo and W. Torruellas, *Spatial solitons*, (Springer-Verlag, Berlin, 2001).
- [2] S. Kivshar and G. P. Agrawal, *Optical Solitons: From Fibers to Photonic Crystals*, (Academic, 2003).
- [3] Y. R. Shen, *The principles of nonlinear optic*, (Wiley & Sons, Inc., New York, 1984).
- [4] C. Rotschild, O. Cohen, O. Manela and M. Segev, Phys. Rev. Lett **95** 213904 (2005).
- [5] P. Zhang, J. L. Zhao, F. J. Xiao, C. B. Lou, J. J. Xu, and Z. G. Chen, Opt. Express. **16**, 3865–3870 (2008).
- [6] F. W. Ye, B. A. Malomed, Y. J. He, and B. Hu, Phys. Rev. A **81**, 043816 (2010).
- [7] Q. Guo and S. Chi, J. Opt. A: Pure Appl. Opt., **2**, 5 (2000).
- [8] S. V. Polyakov and G. I. Stegeman, Phys. Rev. E, **66**, 046622 (2002).
- [9] C. Conti, M. Peccianti, and G. Assanto, Phys. Rev. E, **72**, 066614 (2005).
- [10] S. Polyakov, R. Malendevich, L. Jankovic, G. Stegeman, Chr. Bosshard, and P. Gunter, Opt. Lett., **27** 1049 (2002).
- [11] R. Malendevich, L. Jankovic, S. Polyakov, R. Fuerst, G. I. Stegeman, Chr. Bosshard, and P. Gunter, Opt. Lett., **27** 631 (2002).
- [12] Z. X. Chen and Q. Guo, Opt. Commun., **284** 3183 (2011).
- [13] A. S. Desyatnikov, D. Buccoliero, M. R. Dennis and Y. S. Kivshar, Phys. Rev. Lett **104** 053902 (2010).
- [14] G. Liang and Q. Guo, Phys. Rev. A, **88**, 043825 (2013).
- [15] D. Anderson, Phys. Rev. A **27**, 3135 (1983).
- [16] G. P. Agrawal, *Nonlinear Fiber Optics* (Academic, 3rd ed, San Diego, 2001), pp. 51-55.